

Exploring Probabilistic Modeling Beyond Domain Generalization for Semantic Segmentation

I-Hsiang Chen^{1,2*,†} Hua-En Chang^{1*} Wei-Ting Chen³ Jenq-Neng Hwang² Sy-Yen Kuo^{1,4}

¹National Taiwan University ²University of Washington ³Microsoft ⁴Chang Gung University

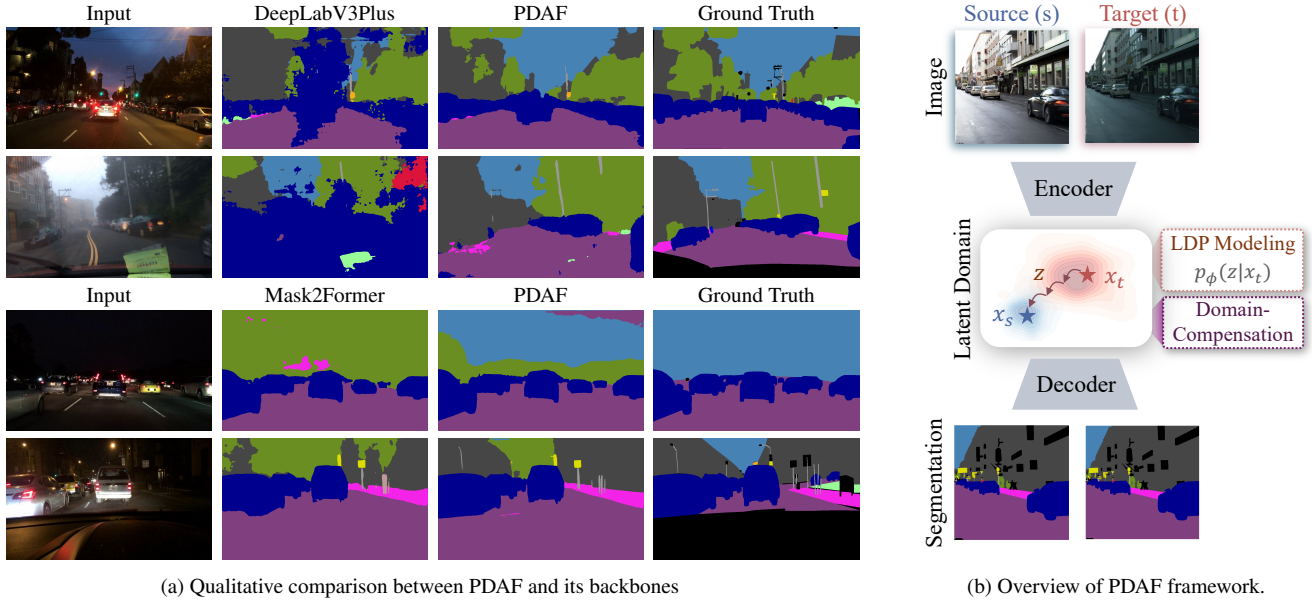


Figure 1. The proposed PDAF enhances existing segmentation backbones (DeepLabV3Plus [7] and Mask2Former [10]) by leveraging latent domain prior modeling as a compensation mechanism, yielding consistent improvements on unseen target domains such as BDD100K [67].

Abstract

Domain Generalized Semantic Segmentation (DGSS) is a critical yet challenging task, as domain shifts in unseen environments can severely compromise model performance. While recent studies enhance feature alignment by projecting features into the source domain, they often neglect intrinsic latent domain priors, leading to suboptimal results. In this paper, we introduce PDAF, a Probabilistic Diffusion Alignment Framework that enhances the generalization of existing segmentation networks through probabilistic diffusion modeling. PDAF introduces a Latent Domain Prior

(LDP) to capture domain shifts and uses this prior as a conditioning factor to align both source and unseen target domains. To achieve this, PDAF integrates into a pre-trained segmentation model and utilizes paired source and pseudo-target images to simulate latent domain shifts, enabling LDP modeling. The framework comprises three modules: the Latent Prior Extractor (LPE) predicts the LDP by supervising domain shifts; the Domain Compensation Module (DCM) adjusts feature representations to mitigate domain shifts; and the Diffusion Prior Estimator (DPE) leverages a diffusion process to estimate the LDP without requiring paired samples. This design enables PDAF to iteratively model domain shifts, progressively refining feature representations to enhance generalization under complex target conditions. Extensive experiments validate the effectiveness of PDAF across diverse and challenging urban scenes.

Project page: <https://pdaf-iccv.github.io>

* Indicates equal contribution.

† This work was conducted while I-Hsiang Chen was an intern at University of Washington.

1. Introduction

Domain Generalized Semantic Segmentation (DGSS) remains a fundamental challenge in computer vision, primarily due to inevitable domain shifts encountered in unseen environments [51, 69]. Segmentation models trained on a source domain frequently degrade on the unseen target domains [2, 8, 37]. This challenge is particularly critical in real-world applications such as autonomous driving [3, 23] and robotic systems [43, 44], where accurate semantic segmentation is essential for ensuring operational safety. Factors such as lighting variations, weather changes, and other underrepresented conditions in training data exacerbate the generalization problem. Addressing the domain shifts thus remains a key obstacle in developing robust and reliable semantic segmentation models.

Within the field of DGSS, two primary methodologies have emerged: data augmentation-based approaches and domain-invariant representation learning-based approaches. Data augmentation-based methods enhance the diversity of training data by introducing synthetic variations, thereby exposing models to a broader spectrum of potential domain shifts and improving their generalization ability [24, 75, 76]. Nevertheless, a crucial limitation of data augmentation-based methods is their significant dependence on auxiliary domains or generation models [18, 29, 39]. Conversely, domain-invariant representation learning methods aim to train models that extract consistent features across different domains, effectively mitigating the impact of domain shift [2, 9, 16, 19, 35, 36, 41, 56]. However, the inherent entanglement between style and content poses a significant challenge, often resulting in the loss of critical semantic information during feature decomposition [1, 26, 66]. Recent works achieve feature alignment by projecting features into a constrained feature space [1, 26, 66], but they often overlook the intrinsic properties of latent domain priors, leading to suboptimal performance [58, 61].

To overcome this limitation, we propose PDAF, a Probabilistic Diffusion Alignment Framework that enhances the generalization of existing segmentation networks through probabilistic diffusion modeling. Specifically, PDAF introduces a Latent Domain Prior (LDP), which models domain-specific variations and guides feature alignment between source and unseen target domains, as illustrated in Figure 1. Specifically, PDAF integrates into a pre-trained segmentation model and leverages paired source and pseudo-target images to simulate domain shifts. This process enables LDP modeling, which serves as a foundation for robust domain alignment. To leverage these priors effectively, PDAF first utilizes the Latent Prior Extractor (LPE) to capture cross-domain relationships between the source and pseudo-target samples, generating an optimal LDP that encodes domain-specific variations. Building upon this, the

Domain Compensation Module (DCM) conditions feature representations on the extracted LDP, ensuring that domain priors guide the adaptation process to mitigate domain shifts while preserving task-relevant information. However, the direct estimation of LDP from explicit source-target pairs may be infeasible in real-world scenarios; to overcome this, the Diffusion Prior Estimator (DPE) employs probabilistic diffusion modeling to infer LDP without requiring paired samples, enhancing the model’s adaptability to unseen domains. Through this progressive refinement, PDAF not only aligns features across domains but also maintains critical variations essential for generalization, leading to improved segmentation performance in complex environments.

Extensive experiments on benchmark datasets validate the effectiveness of PDAF, demonstrating that probabilistic modeling of LDP successfully enhances the domain generalization of existing segmentation networks.

Our main contributions are as follows:

- We introduce PDAF, a novel probabilistic diffusion alignment framework that leverages probabilistic diffusion modeling of latent domain priors (LDP) to enhance the robustness of existing segmentation models against unseen domain shifts.
- We propose three components for PDAF: the latent prior extractor, the domain compensation module, and the diffusion prior estimator. These modules collectively estimate and leverage the LDP for robust feature alignment between source and unseen target domains.
- Extensive experiments across diverse datasets and degradation scenarios demonstrate that our method effectively improves the domain generalization of two widely adopted segmentation models (*e.g.*, DeepLabV3Plus [7] and Mask2Former [10]), achieving state-of-the-art performance.

2. Related Work

Domain Generalized Semantic Segmentation. Domain Generalized Semantic Segmentation (DGSS) enhances model robustness to unseen domains without requiring target data. Existing approaches fall into data augmentation-based methods and domain-invariant representation learning-based methods.

Data augmentation-based methods improve generalization by synthesizing or randomizing styles. DRPC [68] enforces pyramid consistency across stylized versions using real images as style references. GTR-LTR [47] replaces source styles with artistic paintings for global and local texture variation, while WildNet [34] enhances feature-level representations with ImageNet [13] as an external data source. Domain-invariant representation learning-based methods remove domain-specific information via normalization and whitening. IBN-Net [45] integrates Instance Normalization (IN) and Batch Normalization (BN) [27],

while Switchable Whitening (SW) [46] adaptively merges whitening and standardization. ISW [11] and DRL [65] reduce style-sensitive covariance components, whereas SHADE [75] and SAN-SAW [48] introduce style hallucination and semantic-aware alignment. HGFormer [15] and CMFormer [5] leverage self-attention’s visual grouping to handle style variations, demonstrating the strengths of transformer-based models.

Recent studies reveal that excessive style regularization can weaken content discrimination. SPC [26] projects target styles into a source-style space, while DPCL [66] applies multi-level contrastive learning on projected source features. BlindNet [1] integrates covariance alignment and semantic consistency contrastive learning to reduce style sensitivity in the encoder while enhancing decoder robustness. In addition, some methods explore Vision Foundation Models (VFM) to improve robustness and transferability in semantic segmentation [4, 62, 72, 73]. Despite progress, DGSS methods focus on feature alignment and augmentation, leaving domain prior modeling underexplored. To bridge this gap, we introduce probabilistic diffusion modeling, enabling structured domain prior estimation and improved generalization to unseen domains.

Diffusion Models. Diffusion models (DMs) [22] have recently gained significant attention for their outstanding performance in generative modeling. By parameterizing a Markov chain and optimizing the variational lower bound on the likelihood function, DMs effectively capture complex data distributions and produce high-quality samples [22, 30, 33, 59, 70, 71, 74], outperforming conventional frameworks like GANs [14]. To reduce computational overhead, LDM [53] and Würstchen [50] conduct the diffusion process in latent space while retaining high-quality outputs. In addition to this, several studies have leveraged DMs to encode prior knowledge that facilitate downstream tasks. For instance, DiffIR [64] introduces a diffusion process applied to a compact image prior representation, enhancing both efficiency and stability under challenging conditions, while CDFormer [38] jointly reconstructs content and degraded representations to improve textural fidelity, and UniRestore [6] further bridges perceptual and task-oriented image restoration by leveraging diffusion priors. These advancements highlight the role of diffusion-based methods in capturing complex data distribution, enhancing robustness and adaptability in generative modeling

Diffusion Models for Domain Generalization. Recent works explore diffusion models for domain generalization in semantic segmentation. DatasetDM [63] synthesizes diverse image-annotation pairs, while DGIInStyle [29] employs semantic guidance to produce consistently paired image-label samples. Gong *et al.* [20] adopt prompt randomization with pretrained diffusion features, and DIFF [28] integrates sampling and fusion from pre-

trained diffusion models to learn universal feature representations. These methods demonstrate the effectiveness of external diffusion-based models in enhancing domain generalization, but they typically incur substantial computational overhead. By contrast, our approach adopts an efficient probabilistic diffusion modeling framework to explicitly model latent domain priors, capturing diverse domain variations without imposing excessive resource demands. Moreover, this design seamlessly integrates with existing segmentation network, enabling robust out-of-distribution performance with minimal additional overhead.

3. Method

We first introduce the Latent Domain Prior (LDP) Modeling (Sec. 3.1), where we formulate domain generalized semantic segmentation (DGSS) as a probabilistic learning problem and derive the variational inference framework for LDP estimation. Based on this, we develop the Probabilistic Diffusion Alignment Framework (Sec. 3.2), which leverages LDPs to model domain shifts and guide the existing segmentation model in adapting feature representations. Finally, we describe Model Optimization (Sec. 3.3), detailing the training objectives and loss functions designed to enhance robust domain generalization.

3.1. Latent Domain Prior Modeling

We propose a probabilistic modeling framework that explicitly integrates LDP to model domain shifts in the DGSS task. By formulating LDP within a variational inference framework, our method enables principled estimation of domain prior that serves as conditioning variables, thereby guiding segmentation models to generalize more effectively on unseen target domains.

Probabilistic Problem Formulation. To generalize across domain shifts, we cast DGSS as a probabilistic learning problem. We introduce a Latent Domain Prior (LDP) as a latent variable z to capture domain-specific variations that are not directly observable. Given the target domain distribution $p(x_t, y_t)$, where y_t denotes the ground truth, we infer z solely from the available target-domain image x_t . Consequently, the prediction function of PDAF is formulated as:

$$p_{\theta, \phi}(y_t|x_t) = \int p_{\theta}(y_t|x_t, z)p_{\phi}(z|x_t)dz, \quad (1)$$

where θ and ϕ represent the parameters of the segmentation model and the network designed to estimate z (i.e., LDP), respectively. By incorporating LDP, PDAF regularizes feature adaptation, consequently mitigating domain shifts and enhancing model robustness.

Variational Inference for LDP Estimation. To facilitate tractable inference of LDP, we introduce a variational posterior $q_{\varphi}(z|x_t, x_s)$ to approximate the true posterior distribution $p(z|x_t, x_s)$, where φ represents the parameters

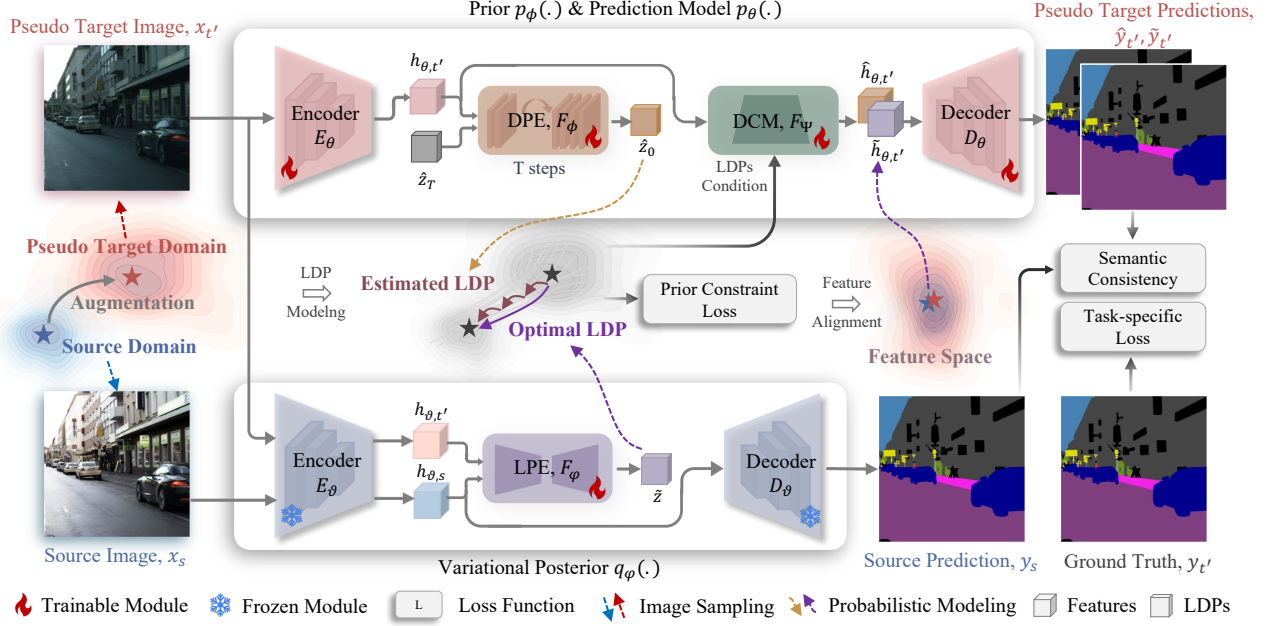


Figure 2. **Overall architecture of PDAF.** PDAF augments a pre-trained segmentation network by introducing LDP modeling to enhance its domain generalization. The LPE learns the optimal LDP by modeling cross-domain relationships between source and pseudo-target domains, while DPE is employed to estimate LDP using only target inputs. Finally, the DCM enhances segmentation network with LDP guidance, refining feature alignment and improving domain generalization.

of the inference network and x_s indicates the source domain counterpart of target domain image x_t . The pair of x_s and x_t preserves semantic consistency while exhibiting domain-specific variations. By leveraging variational inference, we construct a principled optimization framework that estimates LDP to enhance domain alignment. The Evidence Lower Bound (ELBO) of the predictive function is formulated as:

$$\log p_{\theta, \phi}(y_t | x_t) \geq \mathbb{E}_{q_\phi(z | x_t, x_s)} [\log p_\theta(y_t | x_t, z)] - \mathbb{KL}[q_\phi(z | x_t, x_s) || p_\phi(z | x_t)]. \quad (2)$$

The variational posterior $q_\phi(z | x_t, x_s)$ explicitly encodes cross-domain feature correlations from source-target pairs, enabling precise modeling of latent domain variation critical for effective generalization. The KL divergence term encourages the learned posterior to approximate the prior, ensuring structured regularization. A detailed derivation of ELBO is provided in the supplementary material.

3.2. Probabilistic Diffusion Alignment Framework

Overview of the Framework. We introduce the Probabilistic Diffusion Alignment Framework (PDAF), which instantiates LDP modeling to obtain domain shift, thereby enhancing generalization performance of segmentation models. To achieve this, PDAF integrates into a pre-trained segmentation model and utilizes paired images generated

through data augmentation, effectively simulating domain shifts. This process preserves semantic consistency while injecting domain-specific variations, thus facilitating the principled ELBO approximation. The optimization function of PDAF is described as follows:

$$\mathcal{L}_{\text{PDAF}} = -\mathbb{E}_{q_\phi(z' | x_{t'}, x_s)} [\log p_\theta(y_{t'} | x_{t'}, z')] + \mathbb{KL}(q_\phi(z' | x_{t'}, x_s) || p_\phi(z' | x_t)), \quad (3)$$

where $x_{t'}$ represents pseudo-target images generated from source images x_s via data augmentation, while $y_{t'}$ is the corresponding ground truth. z' denotes the LDP, inferred through cross-domain relationships between source and pseudo-target domain samples. The prediction model $p_\theta(\cdot)$, variational posterior $q_\phi(\cdot)$ and prior $p_\phi(\cdot)$ jointly optimize segmentation accuracy while modeling domain shifts by maximizing likelihood and minimizing KL divergence, respectively.

Corresponding to the optimization function in Eq. 3, PDAF introduces three components: (i) a Latent Prior Extractor (LPE), which serves as $q_\phi(\cdot)$ and infers the optimal LDP from source and pseudo-target pairs; (ii) a Domain Compensation Module (DCM), integrated into a pretrained segmentation network to implement the prediction model $p_\theta(\cdot)$, which leverages the extracted LDP to refine feature representations, thereby mitigating domain shifts and improving segmentation accuracy; and (iii) a Diffusion Prior Estimator (DPE), implementing $p_\phi(\cdot)$ through probabilistic

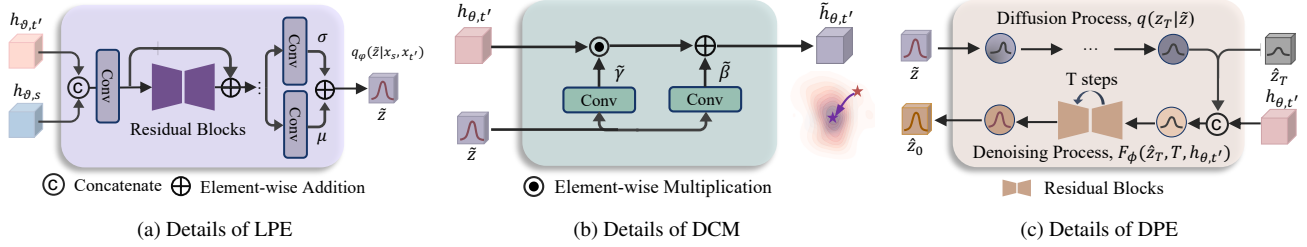


Figure 3. **Schematic diagrams of (a) the Latent Prior Extractor, (b) the Domain Compensation Module and (c) the Diffusion Prior Estimator.**

diffusion modeling to estimate LDP without paired source and target data. Notably, PDAF is compatible with any existing segmentation model, allowing frozen pre-trained encoders E_{ϑ} and decoders D_{ϑ} to discover LDP, and then fine-tuning the target network E_{θ} and D_{θ} for DGSS. The overall architecture of PDAF is illustrated in Figure 2.

Latent Prior Extractor. The LPE is designed to estimate the optimal LDP by supervising cross-domain feature relationships, providing effective guidance for feature alignment. As illustrated in Figure 3a, the LPE first concatenates source features $h_{\vartheta,s}$ and pseudo-target features $h_{\vartheta,t'}$, then utilizes residual blocks to model cross-domain feature relationships. The extracted features are then processed through two projection layers to derive the probabilistic modeling parameters, namely the mean (μ) and variance (σ). To ensure stable and effective training, we constrain the optimal LDP \tilde{z} to follow a standard normal distribution [32], enhancing latent space regularization and enabling more robust prior estimation. The procedure can be formulated as:

$$\begin{aligned} h_{\vartheta,s} &= E_{\vartheta}(x_s), h_{\vartheta,t'} = E_{\vartheta}(x_{t'}), \\ \mu, \sigma &= F_{\varphi}(h_{\vartheta,s}, h_{\vartheta,t'}), \\ \tilde{z} &= \mu + \epsilon\sigma, \epsilon \sim \mathcal{N}(0, I), \end{aligned} \quad (4)$$

where F_{φ} indicates LPE parameterized by φ . The dimension of LDP is $\tilde{z} \in \mathbb{R}^{c' \times h \times w}$, where c' denotes a predefined number of the channel of LDP and h, w correspond to the spatial dimensions of the feature maps.

Domain Compensation Module. The DCM enhances segmentation models for domain generalization. Drawing inspiration from Spatial Feature Transformation (SFT) [60], DCM leverages LDP as a compensation mechanism, providing domain-aware modulation to improve feature alignment. As illustrated in Figure 3b, a straightforward approach involves projecting LDP onto affine transformation parameters using dedicated projection layers (F_{Ψ}), yielding scale ($\tilde{\gamma}$) and shift ($\tilde{\beta}$) parameters. These parameters are then used to rescale and shift the feature representations, effectively normalizing domain discrepancies across spatial regions. The refined features $\tilde{h}_{\theta,t'}$ are subsequently pro-

cessed by the segmentation head D_{θ} to generate accurate segmentation maps $\tilde{y}_{t'}$. The process can be formulated as:

$$\begin{aligned} \tilde{\gamma}, \tilde{\beta} &= F_{\Psi}(\tilde{z}), \\ \tilde{h}_{\theta,t'} &= \tilde{\gamma} \odot h_{\theta,t'} \oplus \tilde{\beta}, \\ \tilde{y}_{t'} &= D_{\theta}(\tilde{h}_{\theta,t'}), \end{aligned} \quad (5)$$

where \odot and \oplus denote element-wise multiplication and element-wise addition, respectively. The dimensions of the affine transformation parameters correspond to the feature map, with $\tilde{\gamma}, \tilde{\beta} \in \mathbb{R}^{c \times h \times w}$.

Diffusion Prior Estimator. Diffusion Models (DMs) have demonstrated their effectiveness in sampling from complex target domains, significantly improving various computer vision tasks as evidenced in previous studies [38, 50, 53]. In DPE, we leverage probabilistic diffusion modeling to estimate the LDP, enabling arbitrary target domain and accurate prior estimation for domain alignment. As illustrated in Figure 3c, we first apply the forward diffusion process to an optimal LDP \tilde{z} , iteratively adding Gaussian noise to obtain an intermediate latent state z_T :

$$q(z_T|\tilde{z}) = \mathcal{N}(z_T; \sqrt{\alpha_T}\tilde{z}, (1 - \alpha_T)I), \quad (6)$$

where $\alpha_T = 1 - \beta_T$ and $\bar{\alpha}_T = \prod_{i=1}^T \alpha_i$. For the reverse diffusion process, the DPE initializes from \hat{z}_T and perform T -step denoising process to estimate the LDP \hat{z}_0 , which is formulated as:

$$\hat{z}_{T-1} = \frac{1}{\sqrt{\alpha_T}}(\hat{z}_T - \epsilon \frac{1 - \alpha_T}{\sqrt{1 - \bar{\alpha}_T}}). \quad (7)$$

Specifically, to estimate LDP for target images, we condition the DPE on the extracted target features $h_{\theta,t'}$. DPE (F_{ϕ}) then performs a denoising operation at timestep T , represented as $F_{\phi}(\hat{z}_T, T, h_{\theta,t'})$. To accommodate the reduced channel dimension of LDP, we employ accelerated diffusion-based optimization [57] for efficient and rapid inference. Moreover, this design allows for the joint training of DPE and the segmentation head D_{θ} , thereby optimizing

LDP directly for the segmentation task. This process is defined as follows:

$$\begin{aligned}\hat{z}_0 &= F_\phi(\hat{z}_T, T, h_{\theta, t'}), \\ \hat{\gamma}, \hat{\beta} &= F_\Psi(\hat{z}_0), \\ \hat{h}_{\theta, t'} &= \hat{\gamma} \odot h_{\theta, t'} \oplus \hat{\beta}, \\ \hat{y}_{t'} &= D_\theta(\hat{h}_{\theta, t'}),\end{aligned}\quad (8)$$

where $\hat{y}_{t'}$ represents the predicted segmentation maps conditions on the estimated LDP \hat{z}_0 . The dimensions of the affine transformation parameters correspond to the feature map, with $\hat{\gamma}, \hat{\beta} \in \mathbb{R}^{c \times h \times w}$.

Inference. During inference, only target domain images x_t are available, so the variational posterior is omitted. Instead, we extract target features $h_{\theta, t}$ using the segmentation backbone $E_\theta(\cdot)$ as the conditioning input and sample a Gaussian noise vector \hat{z}_T . The DPE then iteratively refines this noise over T denoising steps to produce the estimated LDP \hat{z}_0 . Finally, the DCM leverages the estimated LDP to refine the feature representations, which are used for robust segmentation prediction.

3.3. Model Optimization

We train our framework by optimizing the likelihood estimation and enforcing posterior regularization to enhance domain generalization, as defined in Eq. (3). To achieve maximum likelihood estimation, we employ task-specific loss functions $\mathcal{L}_{\text{task}}$ tailored to different segmentation models. Specifically, we use weighted cross-entropy loss for DeepLabV3+ [7] and focal loss for Mask2Former [10]. To further enhance feature consistency, we introduce a semantic consistency loss \mathcal{L}_{sc} that measures the discrepancy between the predictions of the source and pseudo-target images. This loss enforces semantic alignment in feature space and accelerates model convergence:

$$\mathcal{L}_{\text{sc}} = \|f_\theta(x_s) - \tilde{y}_{t'}\|_2 + \|f_\theta(x_s) - \hat{y}_{t'}\|_2, \quad (9)$$

where f_θ denotes the frozen segmentation network $E_\theta(\cdot)$ and $D_\theta(\cdot)$, $\tilde{y}_{t'}$ and $\hat{y}_{t'}$ represent the predictions from Eq. (5) and Eq. (8), respectively. To minimize the KL divergence and enforce posterior regularization, we adopt a prior constraint loss $\mathcal{L}_{\text{prior}}$ to align the outputs of LPE and DPE, thereby implicitly reducing the distributional discrepancy between the posterior and the prior:

$$\mathcal{L}_{\text{prior}} = \|\hat{z}_0 - \tilde{z}\|_2. \quad (10)$$

where \hat{z}_0 and \tilde{z} indicate the optimal LDP and estimated LDP from Eq. (4) and Eq. (8), respectively. The overall loss is:

$$\mathcal{L}_{\text{total}} = \lambda_{\text{task}}\mathcal{L}_{\text{task}} + \lambda_{\text{sc}}\mathcal{L}_{\text{sc}} + \lambda_{\text{prior}}\mathcal{L}_{\text{prior}}, \quad (11)$$

where λ_{task} , λ_{sc} , and λ_{prior} represents the scaling factors.

4. Implementation Details

4.1. Datasets

We conduct experiments on five urban scene semantic segmentation datasets that share 19 common scene categories. **Cityscapes (C)** [12] consists of high-resolution images captured from 50 distinct cities, where we exclusively use the finely annotated subset containing 2,975 training and 500 validation images.

BDD-100K (B) [67] provides 7,000 training images and 1,000 validation images collected from various locations conditions.

Mapillary (M) [42] is a large-scale dataset containing 25,000 high-resolution street-view images sourced globally. **GTA5 (G)** [52] includes 24,966 images simulated using the Grand Theft Auto V game engine, divided into 12,403 training, 6,382 validation, and 6,181 testing samples.

SYNTHIA (S) [54] consists of 9,400 photorealistic synthetic images, including 2,830 for testing.

4.2. Evaluation Protocols

Following existing DGSS benchmarks [1, 11, 15, 45, 46, 49], we adopt a single-source domain generalization setting, where one dataset is used for training (source domain), and the remaining four datasets are treated as unseen target domains for evaluation. For a fair comparison, all experiments are built on DeepLabV3Plus [7] (with ResNet-50 [21]) and Mask2Former [10] (with Swin-T and Swin-L [40]). We use the mean intersection over the union (mIoU) [17] to measure the performance of segmentation.

4.3. Training Details

To facilitate a fair evaluation, we exclusively employ Photometric Augmentation as the data augmentation strategy to generate pseudo-target domain samples. The model is trained with Adam Optimizer [31] with an initial learning rate of 1×10^{-5} , momentum parameters $(\beta_1, \beta_2) = (0.9, 0.999)$, and a batch size of 4 for 100 epochs. The channel of LDP is set to $c' = 4$. In DPE, we adopt a total diffusion timestep of $T = 4$, with the noise variance β_t linearly increasing from $\beta_1 = 0.1$ to $\beta_T = 0.99$. The loss coefficients are adjusted to $(\lambda_{\text{task}}, \lambda_{\text{sc}}, \lambda_{\text{prior}}) = (0.5, 0.5, 1.0)$, balancing the contributions of different loss terms. All experiments are implemented in PyTorch and conducted on a single NVIDIA RTX 4090 GPU. More details of the implementation and hyperparameters analysis are provided in the Supplementary Material.

5. Experiments

5.1. Comparison with State-of-the-arts

To access the effectiveness of PDAF, we compare our approach against a comprehensive set of state-of-the-art meth-

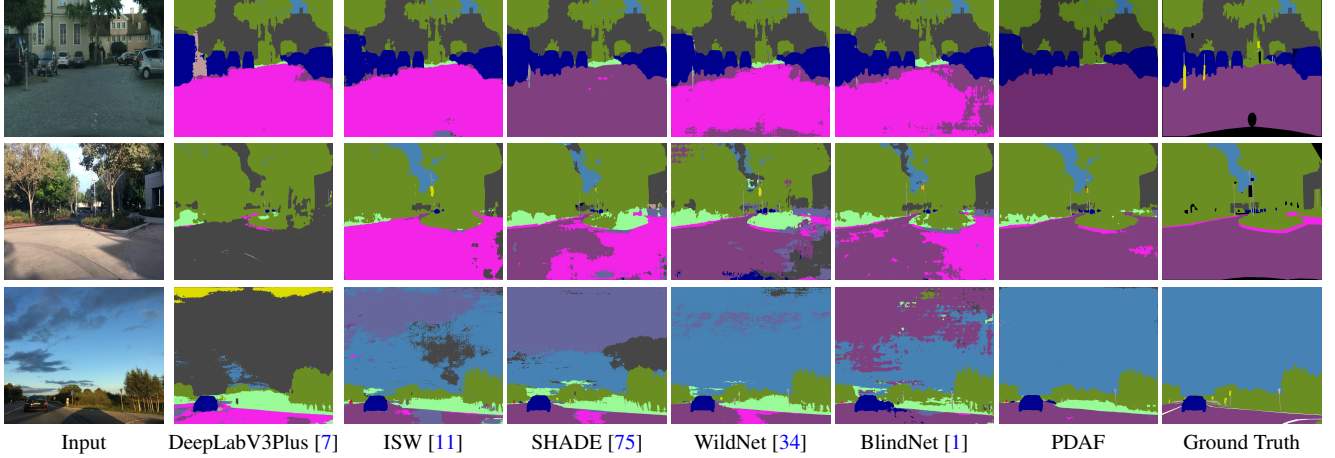


Figure 4. **Qualitative comparison between DGSS methods trained on GTAV (G) [52] using DeepLabV3Plus [7] with ResNet-50 [21].** The first, second, and third rows show the predictions for Cityscapes (C) [12], BDD-100K (B) [67], and Mapillary (M) [42], respectively.

Method	Backbone	Trained on Cityscapes (C)				
		B	M	G	S	Avg.
DeepLabV3Plus [7]	Res50	44.96	51.68	42.55	23.29	40.62
IBN [45]		48.56	57.04	45.06	26.14	44.20
IW [46]		48.49	55.82	44.87	26.10	43.82
Iternorm [25]		49.23	56.26	45.73	25.98	44.30
DRPC [68]		49.86	56.34	45.62	26.58	44.60
ISW [11]		50.73	58.64	45.00	26.20	45.14
GTR [47]		50.75	57.16	45.79	26.47	45.04
DURL [65]		51.80	-	46.52	26.50	-
SHADE [75]		50.95	60.67	48.61	27.62	46.96
SAW [48]		52.95	59.81	47.28	28.32	47.09
WildNet [34]		50.94	58.79	47.01	27.95	46.17
DPCL [66]		50.97	58.59	46.00	25.85	45.34
BlindNet [1]		51.84	60.18	47.97	28.51	47.13
PDAF		53.50	62.93	50.54	30.68	49.41
Mask2Former [10]	Swin-T	51.30	65.30	50.60	34.00	50.30
HGFormer [15]		53.40	66.90	51.30	33.60	51.30
PDAF	Swin-L	56.40	66.40	55.20	34.80	53.20
Mask2Former [10]		60.10	72.20	57.80	42.40	58.13
HGFormer [15]		61.50	72.10	59.40	41.30	58.58
CMFormer [5]		62.60	73.60	60.70	43.00	59.98
PDAF		63.00	74.10	63.20	44.00	61.08

Table 1. **Comparison with existing methods trained on Cityscapes (C) [12].** The best and second-best mIoU scores are blue and magenta.

ods including both CNN-based techniques [1, 7, 11, 25, 26, 34, 45–48, 65, 66, 68, 75, 76] and Mask2Former-based approaches [5, 10, 15]. We adhere to standard DGSS evaluation protocols and report results directly cited from prior works [1, 5, 11, 46, 48].

Cityscapes Source Domain. Table 1 shows that PDAF achieves the best overall performance across four unseen datasets, demonstrating strong generalization to diverse domains. PDAF effectively transfers from real-world datasets (C) [12] to target domains with distinct visual distributions, such as game-rendered synthetic scenes (G) [52] and photo-realistic simulations (S) [54]. Notably, PDAF consistently improves performance across CNN-based and

Method	Trained on GTAV (G)				
	C	B	M	S	Avg.
DeepLabV3Plus [7]	28.95	25.14	28.18	26.23	27.13
IBN [45]	33.85	32.30	37.75	27.90	32.95
IW [46]	29.91	27.48	29.71	27.61	28.68
Iternorm [25]	31.81	32.70	33.88	27.07	31.37
DRPC [68]	37.42	32.14	34.12	28.06	32.94
ISW [11]	36.58	35.20	40.33	28.30	35.10
GTR [47]	37.53	33.75	34.52	28.17	33.49
DURL [65]	41.04	39.15	41.60	-	-
SHADE [75]	44.65	39.28	43.34	-	-
SAW [48]	39.75	37.34	41.86	30.79	37.44
WildNet [34]	44.62	38.42	46.09	31.34	40.12
AdvStyle [76]	39.62	35.54	37.00	-	-
SPC [26]	44.10	40.46	45.51	-	-
DPCL [66]	44.74	40.59	46.33	30.81	40.62
BlindNet [1]	45.72	41.32	47.08	31.39	41.38
PDAF	45.40	43.56	49.45	32.98	42.85

Table 2. **Comparison with existing DGSS methods using a CNN-based network trained on GTAV (G) [52].**

Mask2Former-based methods, highlighting its flexibility in enhancing existing segmentation networks.

GTAV Source Domain. Table 2 demonstrates the effectiveness of PDAF in bridging the domain gap between synthetic and real-world datasets. Unlike existing DGSS methods that rely primarily on feature normalization, PDAF explicitly models latent domain priors, providing structured guidance for feature alignment and enhancing domain generalization. As shown in Figure 4, qualitative comparisons indicate that PDAF effectively preserves detailed structural information—such as road boundaries and object contours—resulting in more precise and consistent segmentation outcomes.

Clear to Corruptions. We evaluate PDAF on ACDC [55], which introduces four real-world adverse conditions (rain,

Method	Backbone	Trained on Cityscape (C)				
		Foggy	Night	Rain	Snow	Avg.
IBN [45]	Res50	63.80	21.20	50.40	49.60	43.70
Iternorm [25]		63.30	23.80	50.10	49.90	45.30
IW [46]		62.40	21.80	52.40	47.60	46.60
ISW [11]		64.30	24.30	56.00	49.80	48.10
PDAF		68.28	30.14	59.23	53.58	52.81
Mask2Former [10]	Swin-T	56.40	39.10	58.90	58.20	53.15
HGFormer [15]		58.50	43.30	62.00	58.30	55.53
PDAF		73.75	47.75	68.12	62.25	62.97
Mask2Former [10]		69.10	53.10	68.30	65.20	63.93
HGFormer [15]	Swin-L	69.90	52.70	72.00	68.60	65.80
PDAF		80.72	55.12	73.13	71.43	70.10

Table 3. Comparison with existing methods evaluated on ACDC [55].

Methods	B	M	G	S	Avg.
Baseline	44.96	51.68	42.55	23.29	40.62
PDAF w/o LPE	49.59	57.63	46.34	27.19	45.19
PDAF w/o DCM	51.51	60.79	49.42	29.55	47.82
PDAF w/o DPE	51.98	60.33	49.38	28.86	47.64
PDAF	53.50	62.93	50.54	30.68	49.41

Table 4. Effectiveness of proposed modules in PDAF.

$\mathcal{L}_{\text{task}}$	\mathcal{L}_{sc}	$\mathcal{L}_{\text{prior}}$	B	M	G	S	Avg.
✓	-	-	49.76	58.73	47.32	27.51	45.83
✓	✓	-	51.28	59.58	48.38	27.94	46.80
✓	-	✓	53.36	62.11	49.69	30.10	48.82
✓	✓	✓	53.50	62.93	50.54	30.68	49.41

Table 5. Analysis on the proposed loss functions.

fog, night and snow). We employ DeepLabV3Plus [7] and Mask2Former [10] as the segmentation network and train our method on Cityscapes [12]. As shown in Table 3, PDAF achieves consistent improvement under all adversarial conditions, demonstrating that LDP effectively compensates for degraded features caused by image corruptions and enhances robustness in varied environments.

5.2. Ablation Studies

To validate the effectiveness of the proposed modules, we perform an ablation study. All experiments are conducted using DeepLabV3Plus [7] with ResNet-50 [21] as the segmentation network. The model is trained on Cityscapes (C) [12] and evaluated on BDD-100K (B) [67], Mapillary (M) [42], GTAV (G) [52], and SYNTHIA (S) [54] to assess generalization across diverse domain shifts.

Effectiveness of Proposed Modules. We consider several experimental configurations: (i) Baseline: vanilla DeepLabV3Plus [7] trained without PDAF; (ii) PDAF w/o LPE: where variational posterior is removed, resulting in LDP estimation without cross-domain guidance; (iii) PDAF w/o DCM: where LDP is directly added to the original features without employing DCM; (iv) PDAF w/o DPE: where DPE is replaced by a single-source LPE, omitting the diffusion process; and (v) PDAF: which integrates all proposed

Number of c'	1	4	16	64	256	1024
Avg. of mIoU	48.74	49.41	48.66	48.35	46.14	45.69

Table 6. Ablation study on the number of channels for LDP.

Number of Steps	1	2	4	8	16	32
Avg. of mIoU	48.88	49.12	49.41	49.43	49.46	49.48

Table 7. Ablation study on the number of timestep in DPE.

modules. As shown in Table 4, each module enhances segmentation performance, with LPE playing a pivotal role in posterior regularization for structured LDP modeling.

Analysis of Loss Functions. Table 5 demonstrates that each loss term contributes to improved performance. The prior constraint loss, $\mathcal{L}_{\text{prior}}$, enforces consistency between the LDPs estimated by LPE and DPE, enabling DPE to accurately infer LDP solely from target samples. Additionally, the semantic consistency loss, \mathcal{L}_{sc} , enhances feature alignment by constraining predictions from both source and pseudo-target samples, further bolstering domain generalization.

Impact of LDP Channel Dimensions. LDP serve as a variational prior for modeling domain shifts while guiding feature alignment in DGSS. The channel dimension of LDP is crucial for capturing domain-specific variations. As shown in Table 6, a channel dimension of 4 yields the best overall performance. In contrast, higher channel dimensions introduce feature redundancy and increase the risk of overfitting, which limits further performance improvements.

Impact of steps for DPE. DPE iteratively refines LDP through the denoising process, facilitating precise alignment across diverse target domains. As shown in Table 7, performance gradually improves with an increasing number of diffusion steps. To achieve an optimal trade-off between efficiency and accuracy, we set the diffusion timestep to 4.

6. Conclusion

This paper introduces PDAF, a probabilistic diffusion alignment framework designed for DGSS. By explicitly modeling latent domain prior (LDP), PDAF captures domain-specific variations to facilitate robust feature alignment across unseen target domains. To achieve this, PDAF involves a latent prior extractor to infer cross-domain relationships, a domain compensation module to condition segmentation features on LDP and a diffusion prior estimator to estimate LDP through a denoising process, allowing robust generalization to unseen domains. Extensive experiments demonstrate the effectiveness of PDAF, improving the generalization of existing segmentation models across diverse environments, highlighting the robustness of LDP modeling in domain generalized semantic segmentation.

Acknowledgements

We thank to National Center for High-performance Computing (NCHC) for providing computational and storage resources. This research was supported by Taiwan's National Science and Technology Council under Grant NSTC 111-2221-E-002-136-MY3 and NSTC 114-2221-E-002-067-MY3.

References

- [1] Woojin Ahn, Geun Yeong Yang, Hyun Duck Choi, and Myo Taeg Lim. Style blind domain generalized semantic segmentation via covariance alignment and semantic consistency contrastive learning. In *CVPR*, 2024. 2, 3, 6, 7
- [2] Yogesh Balaji, Swami Sankaranarayanan, and Rama Chellappa. Metareg: Towards domain generalization using meta-regularization. In *NeurIPS*, 2018. 2
- [3] Florent Bartoccioni, Éloi Zablocki, Andrei Bursuc, Patrick Pérez, Matthieu Cord, and Karteek Alahari. Lara: Latents and rays for multi-camera bird's-eye-view semantic segmentation. In *Conference on robot learning*, 2023. 2
- [4] Yasser Benigim, Subhankar Roy, Slim Essid, Vicky Kalogeiton, and Stéphane Lathuilière. Collaborating foundation models for domain generalized semantic segmentation. In *CVPR*, 2024. 3
- [5] Qi Bi, Shaodi You, and Theo Gevers. Learning content-enhanced mask transformer for domain generalized urban-scene segmentation. In *AAAI*, 2024. 3, 7
- [6] I Chen, Wei-Ting Chen, Yu-Wei Liu, Yuan-Chun Chiang, Sy-Yen Kuo, Ming-Hsuan Yang, et al. Unirestore: Unified perceptual and task-oriented image restoration model using diffusion prior. In *CVPR*, 2025. 3
- [7] Liang-Chieh Chen, George Papandreou, Florian Schroff, and Hartwig Adam. Rethinking atrous convolution for semantic image segmentation. *arXiv preprint arXiv:1706.05587*, 2017. 1, 2, 6, 7, 8
- [8] Wei-Ting Chen, I-Hsiang Chen, Chih-Yuan Yeh, Hao-Hsiang Yang, Hua-En Chang, Jian-Jiun Ding, and Sy-Yen Kuo. Rvsl: Robust vehicle similarity learning in real hazy scenes based on semi-supervised learning. In *ECCV*, 2022. 2
- [9] Wei-Ting Chen, I-Hsiang Chen, Chih-Yuan Yeh, Hao-Hsiang Yang, Jian-Jiun Ding, and Sy-Yen Kuo. Sjd-vehicle: Semi-supervised joint defogging learning for foggy vehicle re-identification. In *AAAI*, 2022. 2
- [10] Bowen Cheng, Ishan Misra, Alexander G. Schwing, Alexander Kirillov, and Rohit Girdhar. Masked-attention mask transformer for universal image segmentation. In *CVPR*, 2021. 1, 2, 6, 7, 8
- [11] Sungha Choi, Sanghun Jung, Huiwon Yun, Joanne T Kim, Seungryong Kim, and Jaegul Choo. Robustnet: Improving domain generalization in urban-scene segmentation via instance selective whitening. In *CVPR*, 2021. 3, 6, 7, 8
- [12] Marius Cordts, Mohamed Omran, Sebastian Ramos, Timo Rehfeld, Markus Enzweiler, Rodrigo Benenson, Uwe Franke, Stefan Roth, and Bernt Schiele. The cityscapes dataset for semantic urban scene understanding. In *CVPR*, 2016. 6, 7, 8
- [13] Jia Deng, Wei Dong, Richard Socher, Li-Jia Li, Kai Li, and Li Fei-Fei. Imagenet: A large-scale hierarchical image database. In *CVPR*, 2009. 2
- [14] Prafulla Dhariwal and Alex Nichol. Diffusion models beat gans on image synthesis. In *NeurIPS*, 2021. 3
- [15] Jian Ding, Nan Xue, Guisong Xia, Bernt Schiele, and Dengxin Dai. Hgformer: Hierarchical grouping transformer for domain generalized semantic segmentation. In *CVPR*, 2023. 3, 6, 7, 8
- [16] Qi Dou, Daniel Coelho de Castro, Konstantinos Kamnitsas, and Ben Glocker. Domain generalization via model-agnostic learning of semantic features. In *NeurIPS*, 2019. 2
- [17] Mark Everingham, S. M. Ali Eslami, Luc Van Gool, Christopher K. I. Williams, John M. Winn, and Andrew Zisserman. The pascal visual object classes challenge: A retrospective. *IJCV*, 2014. 6
- [18] Yaroslav Ganin and Victor Lempitsky. Unsupervised domain adaptation by backpropagation. In *ICML*, 2015. 2
- [19] Muhammad Ghifary, W. Kleijn, Mengjie Zhang, and David Balduzzi. Domain generalization for object recognition with multi-task autoencoders. In *ICCV*, 2015. 2
- [20] Rui Gong, Martin Danelljan, Han Sun, Julio Delgado Mangas, and Luc Van Gool. Prompting diffusion representations for cross-domain semantic segmentation. *arXiv preprint arXiv:2307.02138*, 2023. 3
- [21] Kaiming He, X. Zhang, Shaoqing Ren, and Jian Sun. Deep residual learning for image recognition. In *CVPR*, 2015. 6, 7, 8
- [22] Jonathan Ho, Ajay Jain, and P. Abbeel. Denoising diffusion probabilistic models. In *NeurIPS*, 2020. 3
- [23] Yihan Hu, Jiazhi Yang, Li Chen, Keyu Li, Chonghao Sima, Xizhou Zhu, Siqi Chai, Senyao Du, Tianwei Lin, Wenhai Wang, et al. Planning-oriented autonomous driving. In *CVPR*, 2023. 2
- [24] Jiaying Huang, Dayan Guan, Aoran Xiao, and Shijian Lu. Fsd: Frequency space domain randomization for domain generalization. In *CVPR*, 2021. 2
- [25] Lei Huang, Yi Zhou, Fan Zhu, Li Liu, and Ling Shao. Iterative normalization: Beyond standardization towards efficient whitening. In *CVPR*, 2019. 7, 8
- [26] Wei Huang, Chang Wen Chen, Yong Li, Jiacheng Li, Cheng Li, Fenglong Song, Youliang Yan, and Zhiwei Xiong. Style projected clustering for domain generalized semantic segmentation. In *CVPR*, 2023. 2, 3, 7
- [27] Sergey Ioffe and Christian Szegedy. Batch normalization: Accelerating deep network training by reducing internal covariate shift. In *ICML*, 2015. 2
- [28] Yuxiang Ji, Boyong He, Chenyuan Qu, Zhuoyue Tan, Chuan Qin, and Liaoni Wu. Diffusion features to bridge domain gap for semantic segmentation. *arXiv preprint arXiv:2406.00777*, 2024. 3
- [29] Yuru Jia, Lukas Hoyer, Shengyu Huang, Tianfu Wang, Luc Van Gool, Konrad Schindler, and Anton Obukhov. Dginstyle: Domain-generalizable semantic segmentation with image diffusion models and stylized semantic control. In *ECCV*, 2024. 2, 3

- [30] Zeyinzi Jiang, Chaojie Mao, Yulin Pan, Zhen Han, and Jingfeng Zhang. Scedit: Efficient and controllable image diffusion generation via skip connection editing. In *CVPR*, 2024. 3
- [31] Diederik P. Kingma and Jimmy Ba. Adam: A method for stochastic optimization. In *ICLR*, 2014. 6
- [32] Diederik P. Kingma and Max Welling. Auto-encoding variational bayes. In *ICLR*, 2013. 5
- [33] Diederik P. Kingma, Tim Salimans, Ben Poole, and Jonathan Ho. Variational diffusion models. *arXiv preprint arXiv:2107.00630*, 2021. 3
- [34] Suhyeon Lee, Hongje Seong, Seongwon Lee, and Euntai Kim. Wildnet: Learning domain generalized semantic segmentation from the wild. In *CVPR*, 2022. 2, 7
- [35] Da Li, Yongxin Yang, Yi-Zhe Song, and Timothy M. Hospedales. Learning to generalize: Meta-learning for domain generalization. In *AAAI*, 2017. 2
- [36] Haoliang Li, Sinno Jialin Pan, Shiqi Wang, and Alex Chichung Kot. Domain generalization with adversarial feature learning. In *CVPR*, 2018. 2
- [37] Ya Li, Xinmei Tian, Mingming Gong, Yajing Liu, Tongliang Liu, Kun Zhang, and Dacheng Tao. Deep domain generalization via conditional invariant adversarial networks. In *ECCV*, 2018. 2
- [38] Qingguo Liu, Chenyi Zhuang, Pan Gao, and Jie Qin. Cdformer: when degradation prediction embraces diffusion model for blind image super-resolution. In *CVPR*, 2024. 3, 5
- [39] Yajing Liu, Shijun Zhou, Xiyao Liu, Chunhui Hao, Baojie Fan, and Jiandong Tian. Unbiased faster r-cnn for single-source domain generalized object detection. In *CVPR*, 2024. 2
- [40] Ze Liu, Yutong Lin, Yue Cao, Han Hu, Yixuan Wei, Zheng Zhang, Stephen Lin, and Baining Guo. Swin transformer: Hierarchical vision transformer using shifted windows. In *ICCV*, 2021. 6
- [41] Saeid Motiian, Marco Piccirilli, Donald A. Adjeroh, and Gianfranco Doretto. Unified deep supervised domain adaptation and generalization. In *ICCV*, 2017. 2
- [42] Gerhard Neuhold, Tobias Ollmann, Samuel Rota Bulò, and Peter Kotschieder. The mapillary vistas dataset for semantic understanding of street scenes. In *ICCV*, 2017. 6, 7, 8
- [43] David Nilsson, Aleksis Pirinen, Erik Gärtner, and Cristian Sminchisescu. Embodied visual active learning for semantic segmentation. In *AAAI*, 2021. 2
- [44] Yuya Onozuka, Ryosuke Matsumi, and Motoki Shino. Autonomous mobile robot navigation independent of road boundary using driving recommendation map. In *Int. Conf. on Intel. Robots and Systems*, 2021. 2
- [45] Xingang Pan, Ping Luo, Jianping Shi, and Xiaoou Tang. Two at once: Enhancing learning and generalization capacities via ibn-net. In *ECCV*, 2018. 2, 6, 7, 8
- [46] Xingang Pan, Xiaohang Zhan, Jianping Shi, Xiaoou Tang, and Ping Luo. Switchable whitening for deep representation learning. In *ICCV*, 2019. 3, 6, 7, 8
- [47] Duo Peng, Yinjie Lei, Lingqiao Liu, Pingping Zhang, and Jun Liua. Global and local texture randomization for synthetic-to-real semantic segmentation. *IEEE TIP*, 2021. 2, 7
- [48] Duo Peng, Yinjie Lei, Munawar Hayat, Yulan Guo, and Wen Li. Semantic-aware domain generalized segmentation. In *CVPR*, 2022. 3, 7
- [49] Duo Peng, Yinjie Lei, Munawar Hayat, Yulan Guo, and Wen Li. Semantic-aware domain generalized segmentation. In *CVPR*, 2022. 6
- [50] Pablo Pernias, Dominic Rampas, Mats L. Richter, Christopher J. Pal, and Marc Aubreville. Wuerstchen: An efficient architecture for large-scale text-to-image diffusion models. *arXiv preprint arXiv:2306.00637v2*, 2023. 3, 5
- [51] Sanqing Qu, Tianpei Zou, Lianghua He, Florian Röhrbein, Alois Knoll, Guang Chen, and Changjun Jiang. Lead: Learning decomposition for source-free universal domain adaptation. In *CVPR*, 2024. 2
- [52] Stephan R. Richter, Vibhav Vineet, Stefan Roth, and Vladlen Koltun. Playing for data: Ground truth from computer games. In *ECCV*, 2016. 6, 7, 8
- [53] Robin Rombach, A. Blattmann, Dominik Lorenz, Patrick Esser, and Björn Ommer. High-resolution image synthesis with latent diffusion models. In *CVPR*, 2021. 3, 5
- [54] Germán Ros, Laura Sellart, Joanna Materzynska, David Vázquez, and Antonio M. López. The synthia dataset: A large collection of synthetic images for semantic segmentation of urban scenes. In *CVPR*, 2016. 6, 7, 8
- [55] Christos Sakaridis, Dengxin Dai, and Luc Van Gool. Acdc: The adverse conditions dataset with correspondences for semantic driving scene understanding. In *CVPR*, 2021. 7, 8
- [56] Seonguk Seo, Yumin Suh, Dongwan Kim, Jongwoo Han, and Bohyung Han. Learning to optimize domain specific normalization for domain generalization. In *ECCV*, 2019. 2
- [57] Jiaming Song, Chenlin Meng, and Stefano Ermon. Denoising diffusion implicit models. *arXiv preprint arXiv:2010.02502*, 2020. 5
- [58] Naveen Venkat, Jogendra Nath Kundu, Durgesh Singh, Ambareesh Revanur, et al. Your classifier can secretly suffice multi-source domain adaptation. *NIPS*, 2020. 2
- [59] Jianyi Wang, Zongsheng Yue, Shangchen Zhou, Kelvin CK Chan, and Chen Change Loy. Exploiting diffusion prior for real-world image super-resolution. *IJCV*, 2024. 3
- [60] Xintao Wang, Ke Yu, Chao Dong, and Chen Change Loy. Recovering realistic texture in image super-resolution by deep spatial feature transform. In *CVPR*, 2018. 5
- [61] Zongbin Wang, Bin Pan, Shiyu Shen, Tianyang Shi, and Zhenwei Shi. Domain generalization guided by large-scale pre-trained priors. *arXiv preprint arXiv:2406.05628*, 2024. 2
- [62] Zhixiang Wei, Lin Chen, Yi Jin, Xiaoxiao Ma, Tianle Liu, Pengyang Ling, Ben Wang, Huaian Chen, and Jinjin Zheng. Stronger fewer & superior: Harnessing vision foundation models for domain generalized semantic segmentation. In *CVPR*, 2024. 3
- [63] Weijia Wu, Yuzhong Zhao, Hao Chen, Yuchao Gu, Rui Zhao, Yefei He, Hong Zhou, Mike Zheng Shou, and Chunhua Shen. Datasetdm: Synthesizing data with perception annotations using diffusion models. *NeurIPS*, 2023. 3

- [64] Bin Xia, Yulun Zhang, Shiyin Wang, Yitong Wang, Xinglong Wu, Yapeng Tian, Wenming Yang, and Luc Van Gool. Diffir: Efficient diffusion model for image restoration. In *ICCV*, 2023. [3](#)
- [65] Qi Xu, Lili Yao, Zhengkai Jiang, Guannan Jiang, Wenqing Chu, Wenhui Han, Wei Zhang, Chengjie Wang, and Ying Tai. Dirl: Domain-invariant representation learning for generalizable semantic segmentation. In *AAAI*, 2022. [3](#), [7](#)
- [66] Liwei Yang, Xiang Gu, and Jian Sun. Generalized semantic segmentation by self-supervised source domain projection and multi-level contrastive learning. In *AAAI*, 2023. [2](#), [3](#), [7](#)
- [67] Fisher Yu, Haofeng Chen, Xin Wang, Wenqi Xian, Yingying Chen, Fangchen Liu, Vashisht Madhavan, and Trevor Darrell. Bdd100k: A diverse driving dataset for heterogeneous multitask learning. In *CVPR*, 2018. [1](#), [6](#), [7](#), [8](#)
- [68] Xiangyu Yue, Yang Zhang, Sicheng Zhao, Alberto L. Sangiovanni-Vincentelli, Kurt Keutzer, and Boqing Gong. Domain randomization and pyramid consistency: Simulation-to-real generalization without accessing target domain data. In *ICCV*, 2019. [2](#), [7](#)
- [69] Haojie Zhang, Yongyi Su, Xun Xu, and Kui Jia. Improving the generalization of segmentation foundation model under distribution shift via weakly supervised adaptation. In *CVPR*, 2024. [2](#)
- [70] Juntao Zhang, Yuehuai Liu, Yu-Wing Tai, and Chi-Keung Tang. C3net: Compound conditioned controlnet for multimodal content generation. In *CVPR*, 2024. [3](#)
- [71] Lvmin Zhang, Anyi Rao, and Maneesh Agrawala. Adding conditional control to text-to-image diffusion models. In *ICCV*, 2023. [3](#)
- [72] Xin Zhang and Robby T Tan. Mamba as a bridge: Where vision foundation models meet vision language models for domain-generalized semantic segmentation. In *CVPR*, 2025. [3](#)
- [73] Dong Zhao, Jinlong Li, Shuang Wang, Mengyao Wu, Qi Zang, Nicu Sebe, and Zhun Zhong. Fishertune: Fisher-guided robust tuning of vision foundation models for domain generalized segmentation. In *CVPR*, 2025. [3](#)
- [74] Shihao Zhao, Dongdong Chen, Yen-Chun Chen, Jianmin Bao, Shaozhe Hao, Lu Yuan, and Kwan-Yee K Wong. Uni-controlnet: All-in-one control to text-to-image diffusion models. *NeurIPS*, 2023. [3](#)
- [75] Yuyang Zhao, Zhun Zhong, Na Zhao, N. Sebe, and Gim Hee Lee. Style-hallucinated dual consistency learning for domain generalized semantic segmentation. In *ECCV*, 2022. [2](#), [3](#), [7](#)
- [76] Zhun Zhong, Yuyang Zhao, Gim Hee Lee, and N. Sebe. Adversarial style augmentation for domain generalized urban-scene segmentation. In *NeurIPS*, 2022. [2](#), [7](#)